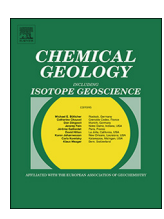


#### Contents lists available at ScienceDirect

### Chemical Geology

journal homepage: www.elsevier.com/locate/chemgeo



## Rapid measurement of strontium in speleothems using core-scanning micro X-ray fluorescence



Nick Scroxton<sup>a,b,\*</sup>, Stephen Burns<sup>a</sup>, Pete Dawson<sup>a</sup>, J. Michael Rhodes<sup>a</sup>, Kaylee Brent<sup>b</sup>, David McGee<sup>b</sup>, Henk Heijnis<sup>c</sup>, Patricia Gadd<sup>c</sup>, Wahyoe Hantoro<sup>d,f</sup>, Mike Gagan<sup>e,f</sup>

- <sup>a</sup> Department of Geosciences, 611 North Pleasant Street, University of Massachusetts, Amherst, MA 01003, USA
- b Department of Earth, Atmospheric and Planetary Sciences, Massachusetts Institute of Technology, 77 Massachusetts Avenue, Cambridge, MA 02139, USA
- <sup>c</sup> Australian Nuclear Science and Technology Organisation (ANSTO), Lucas Heights, NSW 2234, Australia
- <sup>d</sup> Research Center for Geotechnology, Indonesian Institute of Sciences, Bandung 40135, Indonesia
- e Research School of Earth Sciences, The Australian National University, Canberra, ACT 2601, Australia
- <sup>f</sup> School of Earth and Environmental Sciences, The University of Queensland, Brisbane, QLD 4072, Australia

#### ARTICLE INFO

# Editor: G. Jerome Keywords: Speleothem Trace elements Strontium XRF Paleoclimate Speleothem mineralogy

#### ABSTRACT

Speleothem trace element ratios such as Mg/Ca and Sr/Ca are increasingly used in speleothem paleoclimatology as a supplement to stable oxygen and carbon isotope ratios as proxies for past variability in the hydrologic system. Using multiple proxies together allows for a better understanding of both the local and distal hydrologic changes recorded in speleothem chemistry, and therefore of changes in past rainfall. Despite the potential benefits, trace element analysis of speleothems has yet to become widespread, which is likely due to the significant time and costs required by traditional trace element analytical techniques. In this study, we present an in-depth investigation into a rapid, relatively non-destructive and competitively priced technique for measuring Sr/Ca in speleothems: Core-Scanning micro X-ray Fluorescence (CS-µXRF).

We show that CS-µXRF reliably and precisely records Sr concentration in speleothems. Ratioed to near-stoichiometric Ca, the Sr/Ca ratio accounts for variations in beam strength and machine settings, producing a more reliable reported measurement for both intra- and inter-run comparisons. CS-µXRF compares favorably with more conventional trace element procedures such as Quadrupole ICP-MS and ICP-AES, giving confidence in the ability of CS-µXRF to produce paleoclimatologically significant Sr/Ca results. We also identify secondary issues relating to speleothem crystallinity, the dominance of Ca spectral peaks, and comparatively lower energy X-rays that can interfere with precise CS-µXRF analyses. If these can be overcome then CS-µXRF may provide an even more useful method of trace element analysis in speleothem studies.

#### 1. Introduction

The principal aim of many speleothem based paleoclimate studies is the reconstruction of past rainfall. The most commonly used speleothem proxy for rainfall is  $\delta^{18}$ O which typically records the intensity of atmospheric convection and the extent of rainout of an airmass as part of the "so-called amount effect" (Risi et al., 2008; Rozanski et al., 1993). The amount effect, however, is seldom the only or even primary control on speleothem  $\delta^{18}$ O, which may also be influenced by air mass trajectory, changing source moisture(s) and in-karst alteration of the environmental signal from rainwater to speleothem calcite (Johnson and Ingram, 2004; Kanner et al., 2012; Lachniet, 2009; LeGrande and Schmidt, 2009, 2006). Like all proxies, speleothem  $\delta^{18}$ O is complex, but is frequently interpreted as a proxy for integrated paleoconvection from

evaporation to precipitation.

As an alternative or complement to  $\delta^{18}$ O, many studies measure concentrations of trace elements such as Mg, Sr, P, U, or their ratios normalized to calcium (Fairchild and Treble, 2009; Jamieson et al., 2016; Treble et al., 2003; Verheyden et al., 2000). In contrast to  $\delta^{18}$ O, which can be affected by processes occurring at great distance from the speleothem, variability in trace elements concentrations are controlled by local variables such as groundwater pH, residence time in the soil and karst, prior calcite precipitation and the evolution of the flow regime. The extent of these processes are highly influenced by changing rainfall and therefore variability in speleothem trace elements can be considered as a proxy for the impacts of local rainfall on the karst hydrology (Baldini et al., 2006; Cruz et al., 2007; Fairchild et al., 2000; Fairchild and Treble, 2009; Johnson et al., 2006).

<sup>\*</sup> Corresponding author at: Department of Geosciences, 611 North Pleasant Street, University of Massachusetts, Amherst, MA 01003, USA. *E-mail address*: nscroxton@umass.edu (N. Scroxton).

With contrasting centers of action, trace elements and  $\delta^{18}O$  are thus highly complementary and an increasing number of studies use a multiproxy approach (Griffiths et al., 2013, 2016; Orland et al., 2014). However, producing multiple time series is expensive. The widespread adoption of trace element analyses requires a method that is accessible and affordable to most speleothem scientists.

X-ray fluorescence (XRF) is a technique for determining elemental abundances in a variety of materials (Ramsey et al., 1995). High energy primary X-rays bombard a sample material to remove inner shell electrons. Outer orbital shell electrons "fall" to the lower energy orbitals, fluorescing characteristic secondary X-rays which are measured. So far. XRF in speleothems has primarily been used in studies using synchrotron radiation (Borsato et al., 2007; Kuczumow et al., 2005, 2003). Synchrotron radiation micro-XRF (SR-µXRF) is a powerful micron scale XRF technique capable of mapping trace element concentrations at 1 ms per pixel, with ppb detection limits and high energy resolution of 0.05 keV (Brown and Sturchio, 2002, Borsato et al., 2007). SR-µXRF has been used on speleothems to determine past volcanism (Badertscher et al., 2014; Frisia et al., 2005, 2008) and track how trace elements move through the karst system (Frisia et al., 2012; Wynn et al., 2012, 2014). While SR-µXRF is highly suited for mapping and high-resolution applications, it has some drawbacks. SR-µXRF requires cutting up samples to be less than  $20 \times 25$  mm for vacuum soft X-ray beam lines or 120 × 80mm for non-vacuum hard X-ray beam lines, multiple runs on different beam-lines for different elements, and prescanning and multiple line scans to avoid lateral heterogeneity. Therefore SR-µXRF may not be suited to producing lengthy records.

The use of low power XRF systems has advantages and disadvantages compared to SR-µXRF. Increased throughput must be traded against decreased energy and spatial resolution, and higher detection limits. de Winter et al. (2017) used a benchtop near-vacuum XRF system to determine concentrations of 21 elements in carbonates, but the vacuum system requires cutting samples to fit the sampling chamber. Non-vacuum XRF allows for larger samples, but the attenuation of secondary X-rays in the air-gap prevents the analysis of lighter elements such as Mg, which attenuates 90% in 1 cm of air. Buckles and Rowe (2016) used a portable XRF system on speleothems, showing non-vacuum XRF to be a viable option for analyzing trace elements in speleothems. In our study, we build on the work of Buckles and Rowe (2016), providing additional internal tests, external comparisons with other methodological techniques, and using a different machine, with greater lateral scan length.

Core-scanning XRF (CS- $\mu$ XRF) is a low power, large chambered, non-vacuum, XRF system. CS- $\mu$ XRF is five to ten orders of magnitude less bright than SR- $\mu$ XRF (Croudace and Rindby, 2006), resulting in decreased energy resolution (100 keV), decreased spatial resolution (100  $\mu$ m) and detection limits 10–20 times higher than conventional pellet-based XRF or SR- $\mu$ XRF (Borsato et al., 2007; Croudace and Rindby, 2006). Yet it has higher throughput and the larger chamber allows for samples up to 1750 mm long, 75 mm wide and 60 mm deep; it is essentially non-destructive for many speleothem samples. If the limitations of CS- $\mu$ XRF do not prevent detection of the desired signal in paleoclimate archives, then CS- $\mu$ XRF has great potential as a paleoclimate tool. Indeed, CS- $\mu$ XRF use is common in paleoclimate archives such as sediment cores.

The use of CS- $\mu$ XRF has yet to make the transition to widespread adoption in the speleothem community. This is largely due to concerns over the crystalline matrix of carbonates generating X-ray diffraction (XRD) peaks, and the presence of a dominant single element, calcium, which results in large, wide  $K\alpha$  and  $K\beta$  peaks plus significant sum and escape lines. These additional peaks interfere with the characteristic XRF peaks of other elements rendering them unresolvable. Further, speleothem trace element concentrations are frequently lower than the detection limits of CS- $\mu$ XRF. Despite potential shortcomings, initial studies using CS- $\mu$ XRF on stalagmites are beginning to produce results. Recent studies have measured Ba/Ca as a vegetation derived proxy for

temperature (Wu et al., 2012), Sr and Sr/Ca as a proxy for wet/dry conditions (Li et al., 2015; Tan et al., 2015), and Fe and Si as indicators of detrital flood layers (Finné et al., 2015).

The question remains as to whether low power CS- $\mu$ XRF can provide a faster, less destructive technique that could lead to more widespread use of XRF in speleothem paleoclimate. In this study, we investigate the use of CS- $\mu$ XRF in speleothems using a Cox Analytical Systems ITRAX core scanner (hereafter Itrax) on stalagmites from Madagascar and Indonesia, with a focus on Sr and the Sr/Ca ratio. We run a series of tests to determine the reproducibility, precision, and quantification of trace element results. Then we compare the results of speleothem scans with mass spectrometry techniques to test the accuracy of CS- $\mu$ XRF against more traditional methods.

#### 2. Methods

Itrax CS- $\mu$ XRF was conducted at the University of Massachusetts Amherst (UMass) and the Australian Nuclear Science and Technology Organisation (ANSTO). Samples at UMass were run with a molybdenum tube at 60 kV and 50 mA. Samples at ANSTO were run with a chromium tube at 40 kV and 45 mA. While both tube types are capable of measuring a full suite of elements, different tubes are appropriate in different situations. The characteristic X-rays produced by a molybdenum tube will have greater excitation efficiency and higher detection limits at the relevant Sr energies at 14.1–14.2(K $\alpha_{1,2}$ ) and 15.8–16.1 keV (K $\beta_{1,2,3}$ ). Chromium tubes are generally used for studies targeting lighter elements. The results from the ANSTO analysis were part of a study which targeted lighter elements.

The Itrax core scanner does not use filters. The spectral fitting software reduces the need to run with multiple settings, allowing a single scan for all elements with no filters. The single scan increases the throughput and decreases cost. The detectors used do not saturate at the calcite peak. The spectral fitting software also accounts for detection limits, reporting only significant peaks in the output. Specific detection limits vary by element, and matrix composition and crystallinity.

The dimensions of the Itrax allow samples up to 1750 mm long, 75 mm wide and 60 mm deep. For smaller diameter speleothems, such as already halved stalagmites, the process can be considered non-destructive. The sample width can be increased to 105 mm with judiciously placed cuts into the back of the stalagmite, and the sample depth to 75 mm with non-standard cradles. The spatial resolution of the Itrax is 0.2 or 0.1 mm depending on the model and is constrained by the beam size. The X-ray beam runs down the center of the sample, producing an illuminated area 16 mm wide. A collimator reduces the width of the beam visible to the detector to 4 mm. The sample cradle can be moved laterally by integer increments of 1 or 2 cm to account for major changes in growth direction, but fine scale adjustments are not possible. Therefore, Itrax analysis may not be suitable for specimens with complicated growth histories, or stalagmites without 16 mm wide, flat growth surfaces.

It is important that the sample is flat and level down-axis as the Itrax requires a flat surface to maintain the distance between the detector and the sample surface, and minimize the dampening effects of the air gap. XRF has a high sensitivity to stalagmite porosity: imperfections such as former inclusions, sampling holes and trenches all interfere with the results. High resolution techniques such as SR-µXRF and Laser Ablation Inductively Coupled Plasma Mass Spectrometry (LA-ICP-MS) require multiple line scans to avoid small imperfections. The 16 mm wide beam of the Itrax should minimize the effect of small-scale lateral heterogeneity, but a flat surface without prior sampling should be used. Where sampling is retrospective, such as in this study, the opposite face of the sampled stalagmite can be used, with care taken over the additional chronological uncertainty. Buckles and Rowe (2016) suggest that samples should be polished, to minimize the impacts of surface roughness on elemental bias, as the characteristic X-rays of lighter elements are emitted from shallow depths. This "information depth",

defined as where 63% of the secondary X-rays escape the matrix, is dependent on several variables including the density, porosity and fabric of the carbonate matrix and the sample geometry. At a 45° beam incidence angle the information depth is around 20  $\mu m$  for Ca and 117  $\mu m$  for Sr. However, the degree to which surface roughness influences the elemental results has not yet fully tested. Since polishing may selectively pluck aragonite or detrital grains biasing the record in other ways, we used smooth (cut with a fine diamond blade) but unpolished surfaces.

In speleothem paleoclimatology Sr/Ca is typically used rather than Sr concentration because comparative ratios better account for machine variability. In speleothems the Ca concentration is very close to stoichiometric and so Sr concentration and Sr/Ca curves appear similar. Sr and Ca have different excitation volumes and therefore may not respond linearly to machine or matrix variability. However, near constant Ca concentration orders of magnitude higher than Sr should result in nearly all variability in the Sr/Ca ratio coming from Sr variability. Additionally, in speleothems the matrix should be near constant (i.e. calcium carbonate) and variations in the mass absorption coefficient should be trivial. Due to these two effects we assume a linear model in our Sr/Ca ratio. However, due to differences in excitation volume and efficiency, the absolute Sr/Ca may not be accurate. As a result, Sr/Ca ratios should be standardized using a set of standards with independently measured concentrations.

To standardize the Itrax record, three matrix matched calcium carbonate in-house standards were created using offcuts from speleothems with contrasting Sr concentrations. CCXS-1 is a clean calcite sample made from a Yucatán stalagmite. CAXS-1 is a clean aragonite sample from the interior of a Madagascan stalagmite. DAXS-1 is a dirty aragonite sample made from the external layers of the same Madagascan stalagmite with notable flood horizons and high detrital content. About 150 g of stalagmite pieces were broken up with a chisel and mortar to pea-sized chunks, before being crushed in a tungsten carbide shaker box for 20 or 30 s (for soft aragonite and harder calcite respectively). This procedure rules out tungsten from the analyzable elements for this sample due to contamination. 10 g of powder was then pressed into pellets using polyvinyl alcohol to bind the powder and six tons of hydraulic pressure, before being baked overnight at 60 °C. The pressed pellets were scanned once per Itrax run, alongside the samples. Additional pellets are available from the author on request.

To determine strontium concentrations of the in-house standards, aliquots of the crushed but non-binded or pressed pellets were analyzed using Q-ICP-MS at the Massachusetts Institute of Technology according to the procedure below. Additionally, pressed pellets were analyzed using conventional XRF on a PANalytical PW2400 XRF spectrometer at the University of Massachusetts Amherst. Intensities were corrected for non-linear backgrounds, inter element interferences and variations in mass absorption coeffections and were calibrated using a series of synthetic and rock standards (Chappell, 1991; Norrish and Chappell, 1967; Rhodes and Vollinger, 2004). Conventional XRF gives Sr concentration with a two standard deviation of 3 ppm. Sr/Ca ratios were calculated using the assumption of low trace element concentration and therefore a close to stoichiometric Ca concentration of 40%, although this assumption may be more accurate for calcite than aragonite (Lachniet, 2015).

We compare our results to more traditional trace element techniques: Quadrupole Inductively Couple Plasma Mass Spectrometry (Q-ICP-MS) and Inductively Coupled Plasma Atomic Emission Spectrometry (ICP-AES). Q-ICP-MS was conducted on powders from stalagmite AB2 from northern Madagascar (Scroxton et al., 2017).  $0.01-2\,\mathrm{mg}$  of powder was dissolved in 300  $\mu$ l of 0.5 ml HNO3 before 50  $\mu$ l aliquots were diluted with 7 ml of 0.5 M HNO3 and analyzed using an Agilent 7900 Q-ICP-MS.  $^{43}\mathrm{Ca}$ ,  $^{44}\mathrm{Ca}$ ,  $^{24}\mathrm{Mg}$  and  $^{88}\mathrm{Sr}$  concentrations were measured and corrected for isotope abundance to give relative elemental concentrations (Fernandez et al., 2011). Barium was measured but not interpreted due to high background. An indium-scandium

solution was used as an internal standard to determine measurement precision and accuracy, alongside a standard solution measured at various dilutions. A mixed standard prepared from Mg, Ca, Sr and Ba standards from Spex CertiPrep was used to assess instrument sensitivity for these elements and track instrument drift. The standard was run at a variety of concentrations spanning the concentrations observed in the samples; changes in elemental ratios as a function of concentration were minimal (< 10%). Replicate Sr/Ca measurements of different dilutions of the same parent solution varied by 1.4% (0.2–1.3%, one outlier at 6.0%).

For mineralogical comparisons, 21 X-ray diffraction (XRD) analyses were conducted on stalagmite AB2. XRD analyses were conducted on a PANalytical X'Pert PW1821 X-ray diffractometer. For select sections of speleothem AB2 with potential recrystallization or areas of mixed mineralogy, visual identification of the mineralogy and fabric was conducted on five 40  $\times$  60 mm thin sections using a light microscope.

#### 3. Results

We present the results of our Itrax experiments as follows: first we assess the output of single and combined Itrax spectra and account for the influence of the calcite matrix and high calcium abundance. From this we deduce which trace elements in speleothems are most suitable for analysis by Itrax CS-µXRF. For the remainder of the paper we focus on Sr and Sr/Ca: first by assessing internal variability and stability associated with Itrax analyses (Section 3.1). We then asses the run-to-run variability and reproducibility (Section 3.2) before comparing our Itrax results with Q-ICP-MS (Section 3.3). In the discussion we apply our Sr/Ca results to two different uses: firstly, as a rapid test of speleothem mineralogy (Section 4.1); secondly, as an indicator of past karst hydrologic conditions, and by extension, past rainfall (Section 4.2).

Each point scan produces a spectrum of counts at different energies (Fig. 1). Determining elemental abundances from each spectrum is calculated from a hypothetical spectrum. In the Q-spec software the user varies the elements chosen and X-ray tube and detector settings to

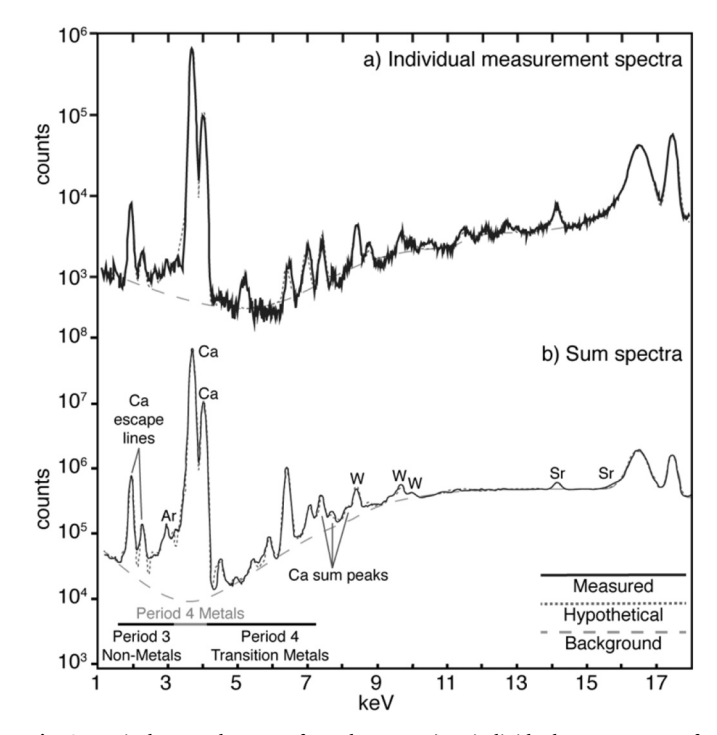


**Fig. 1.** Typical spectral outputs from the Itrax: a) an individual measurement of a stalagmite, b) a sum spectra from in-house standard DAXS-1. Solid line: measured spectra. Dotted line: hypothetical spectra derived from the suite of elements chosen by the user. Dashed line: background.

produce a hypothetical spectrum that closely matches the observed spectrum. In most cases, the sum spectra from the entire scan is used. Sum spectra are the sum of all spectra in a scan and, due to the higher number of overall counts, provide a better signal to noise ratio to resolve smaller peaks. The hypothetical spectrum is then matched to the rest of the individual spectra to produce quantified counts per second per milliamp for each element selected for each point scan.

For speleothems, there are several complicating factors that make this process non-trivial: the dominance of very large calcium spectral peaks, false peaks arising from diffraction and machine parts, and continuous versus discrete abundances relative to the detection limits. Owing to the high Ca concentration in speleothems, Ca peaks dominate the spectra, including two major Ca  $K\alpha_{2,1}$  and  $K\beta_{1,3}$  peaks at 3.69 and 4.01 keV, three sum peaks at 7.38 ( $K\alpha+\alpha$ ), 7.70 ( $K\alpha+\beta$ ) and 8.02 ( $K\alpha+\beta$ ) keV and two escape peaks at 1.95 and 2.27 keV (e.g. Fig. 1). These large peaks obscure many elements that have characteristic peaks with similar keV, e.g. P, S, Cl, K and V, all of which might contain paleoclimate information.

False peaks can be introduced to each spectrum by X-ray diffraction of the carbonate lattice. Diffraction peaks frequently have a shifting keV due to subtle down-core differences in the angle of scattering by the carbonate lattice. Spurious diffraction peaks can therefore be recognized by a drift in peak location from sample to sample. However, in sum spectra they can result in a single peak which can be falsely attributed to an element. Over-matching the suite of elements in data analysis software can then attribute these peaks to an element not found in the speleothem. For example, in this study we note a peak in the sum spectra of many of the analyzed speleothems located close to the Yb  $L\alpha$ peak of 7.42 keV. The addition of Yb to the hypothetical spectrum improves the statistical fit, but gives an unreasonably large Yb concentration. By "solving" one false peak, additional smaller false peaks are introduced at other Yb characteristic voltages. Care must be taken not to identify elements which are unlikely to exist in significant concentrations in the stalagmite just for the sake of improving the statistical match. Some a priori knowledge of the stalagmite or dripwater trace element composition is beneficial here.

Additional false peaks can also be introduced from elements involved in the working of the Itrax. Peaks arise from Ar in the air-gap between sample and detector, W, Ta, Pt and Au peaks can all arise from the core-scanner, Mo or Cr from the X-ray tube, and Ca escape lines from the Si detector. While these peaks should be included in the hypothetical spectra, these elements should not be interpreted as arising from the stalagmite sample.

The use of sum spectra to produce a hypothetical spectrum is convenient and quick but may not detect all elements present. The initial peak matching process only identifies elements whose average composition is above the detection limits. Elements whose concentrations only exceed the minimum detection limits in spikes, such as at hiatuses or detrital layers, can either be detected later when applying the hypothetical spectrum to each individual analysis or can be assumed to be present even if they contribute little or nothing to the sum spectra. CS- $\mu XRF$  of speleothems has excellent potential as a tool for detecting flood layers or hiatuses in speleothems (Finné et al., 2015).

Despite such caveats, there are elements which are reliably detected by CS- $\mu$ XRF, although the particular set of such elements for a given stalagmite is likely to be highly dependent on the chemistry of its drip site. The elements which hold the most promise in providing reliable results include the period 4 transition metals (e.g. V, Ni, Cu), which may relate to organic matter through colloidal transport (Blyth et al., 2016), and strontium, a well-studied element in the karst system. Sr is typically interpreted as varying with the degree of prior calcite precipitation in the karst, and therefore as a proxy for groundwater residence time and paleohydrology. Through XRF, Sr produces characteristic peaks at  $14.1-14.2(K\alpha_{1,2})$  and 15.8-16.1 keV(K $\beta_{1,2,3}$ ), well away from interference by calcium, diffraction peaks, or other elements typically found in high abundance in speleothems. Therefore, Sr is a

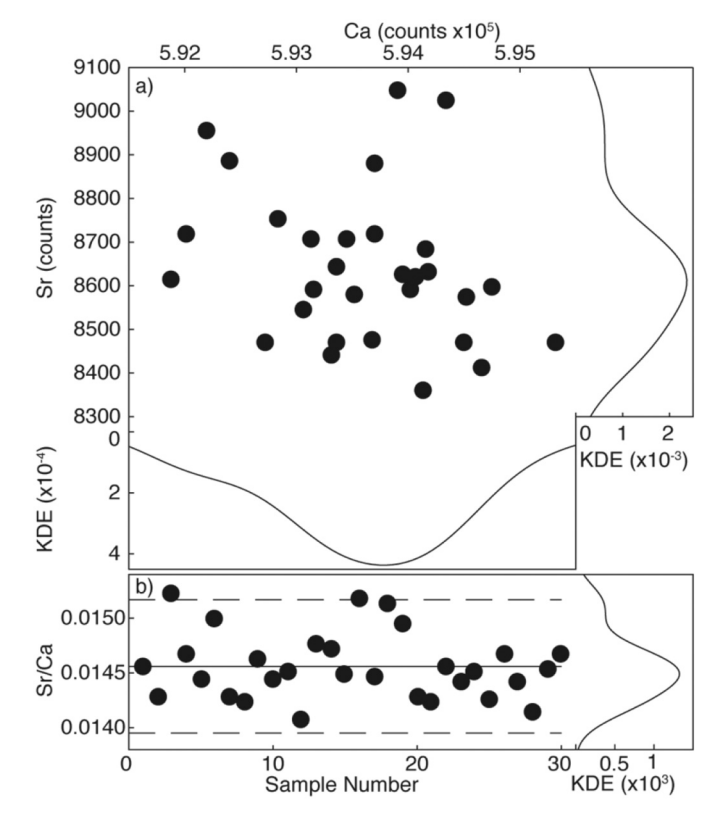


Fig. 2. a) Counts of strontium and calcium for 30 consecutive measurements of the same spot at 40 s count time. b) Sr/Ca ratios from the results in a) with solid and dashed lines indicating mean and two standard deviations of the Sr/Ca ratio. Alongside each plot the kernel density estimates (KDE) of each distribution.

promising first element to use in evaluating the potential of CS-µXRF in speleothem studies. For the rest of this paper we focus on the Sr results.

#### 3.1. Intra-run reproducibility

Itrax stability was tested by analyzing the same spot 30 consecutive times using a 40-s count time (Fig. 2). The distribution of Sr, Ca and Sr/Ca are expected to form a Poisson distribution (Buckles and Rowe, 2016), but are also statistically indistinguishable from a normal distribution. Sr counts had a 2-standard deviation range (2 $\sigma$ ) of 354 counts or 4.1% of the total. Ca counts had a 2 $\sigma$  range of 1675 counts, 0.3% of the total, and the combined Sr/Ca ratio had a 2 $\sigma$  range of 0.0006 or 4.2%, confirming that variability in the Sr/Ca ratio arises predominantly from Sr. This value compares favorably with the overall range of Sr/Ca observed in a 60 mm long repeated transect of 0.014. Of the variability encountered, there was no significant trend between the two counts (p = 0.93) suggesting that systematic variation such as in beam strength is unlikely to be the cause of the count variability.

We tested the reproducibility of the stalagmite signal and the impact of count times using repeated scans of the same 60 mm long transect (Fig. 3). Intra-run reproducibility was tested with five sets of three scans conducted at 10, 20, 40, 60 and 120 s count times. The peak areas and total numbers of Sr and Ca counts were proportional to the count time, with no consistent change in the number of counts per second with count time. Converting elemental counts to Sr/Ca ratio (Fig. 3b) produces no systematic offset between scan times, with all major features of 60 mm long record visible at all count times. Therefore, we conclude that the Sr/Ca ratio in stalagmites can be reliably recorded at count times as low as  $10 \, \text{s}$ .

While the main features of the Sr/Ca record are detectable at  $10\,s$  count times, there is considerable uncertainty which decreases with

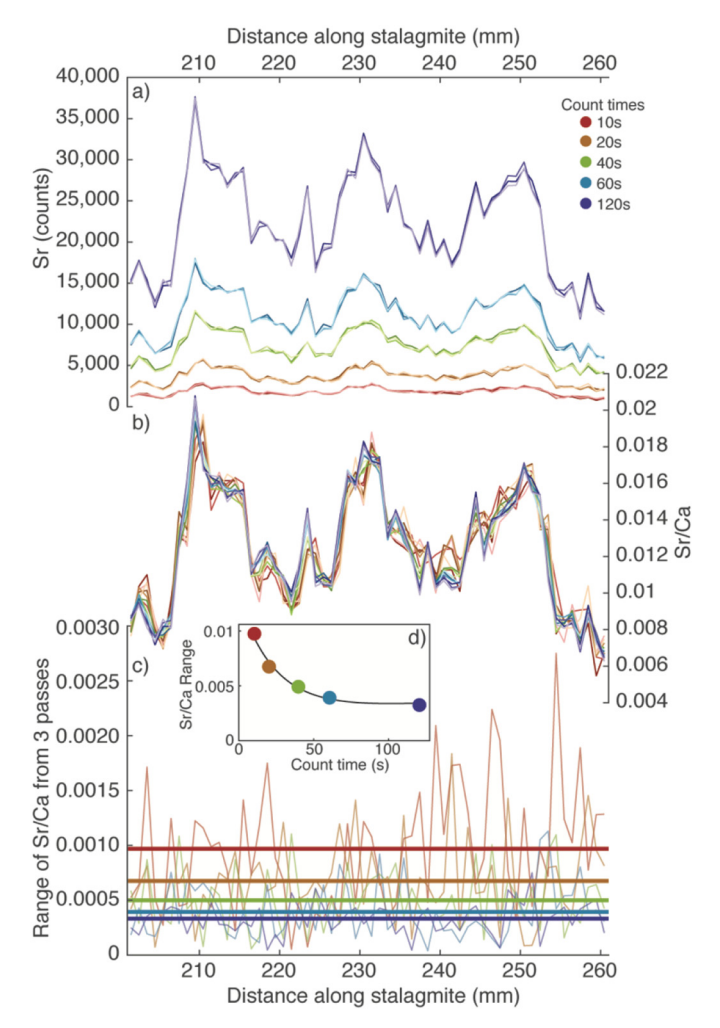


**Fig. 3.** Intra-run reproducibility of a) Sr counts and b) Sr/Ca ratio from 3 separate runs of five different count times: 10 s (red), 20 s (orange), 40 s (green), 60 s (blue), 120 s (purple). c) 60 ranges of three Sr/Ca results per count time per data point (light colors), with the mean of all 60 ranges per count time (solid bar). d) Sr/Ca range plotted against count time (colored circles) with a two-term exponential fit (black). (For interpretation of the references to color in this figure legend, the reader is referred to the web version of this article.)

increasing count time due to better counting statistics. The interaction between X-rays and electrons in the sample is a random, independent event and therefore a Poisson process. The error on an Itrax peak should therefore be equivalent to the square root of the peak area. The longer the count-time, the smaller the relative uncertainty (Croudace and Rindby, 2006; Jarvis et al., 2015). Although three consecutive scans are insufficient to produce meaningful statistics, there is a decreasing range of values with increasing count time, and therefore decreasing error (Fig. 3c). The benefit of increasing count time is reduced with very long count times, such that a 120 s count time produces little extra certainty in the Sr/Ca result (Fig. 3d). Increasing count time increases the whole scan time and therefore instrument costs. Therefore, we suggest a 40 s count time provides a good balance between uncertainty and cost at approximately \$2.50 per data point.

While 40 s count times produce a good balance between duration and precision it may be that longer scans are required for accurate quantified results. de Winter et al. (2017), using a bench-top XRF system, showed that count times above 60 s are required to produce results that are both precise, inside the error of measured certified standards, and accurate, also matching the absolute Sr/Ca value of the standard. With increasing analysis time Sr/Ca ratios approach the measured standard value asymptotically from lower Sr/Ca, principally

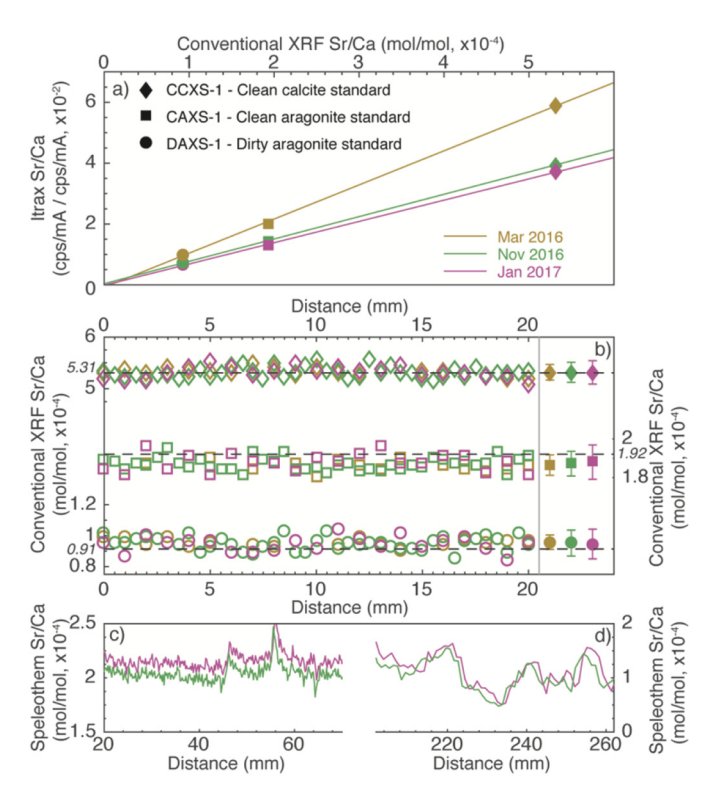


Fig. 4. Correction of Itrax XRF Sr/Ca ratios (cps/mA/cps/mA) to mol/mol ratios using in-house carbonate matrix standards measured on conventional XRF and ICP-MS. a) Sr counts measured on the Itrax versus Sr/Ca ratio calculated using Sr concentration (ppm) from conventional XRF and an assumption of stoichiometric 40% Ca concentration. b) line scan measurements of in-house standards testing standard homogeneity. Open symbols indicate line scans, closed symbols show the mean of each line scan with  $2\sigma$  error bars. c) Inter-run variability of Sr (ppm) concentrations on the same sections of stalagmite AB2 as Fig. 4. In all panels a dark yellow color represents the machine run during March 2016, green, November 2016, and purple, January 2017. Diamonds indicate measurements of the in-house standard CCXS-1, squares, CAXS-1, and circles, DAXS-1. (For interpretation of the references to color in this figure legend, the reader is referred to the web version of this article.)

due to improved counting statistics on the smaller Sr peak. The lack of a systematic trend of increasing Sr/Ca with increased count time in our results suggests that any such effect is within error of our analytical setup.

#### 3.2. Inter-run reproducibility

To test the effects of inter-run variability, we analyzed a set of carbonate matrix in-house standards and Madagascan stalagmite AB2 several times over the course of 13 months. While the major features of the Sr and Sr/Ca records are captured successfully from run to run, there is an absolute offset in Sr counts between different runs on different days. Conversion of Sr counts to Sr/Ca removes a significant amount of inter-run variability, therefore the cause of inter-run variability appears to affect each element similarly. However, there are still some days which produce offsets even in Sr/Ca (Fig. 4a). The causes of inter-run variability are uncertain, but could relate to changing X-ray tube performance/degradation, humidity in the air gap etc.

Variable Sr/Ca ratios from run to run necessitates the use of standards to produce replicable results. We tested the in-house standards using multiple methodologies to assess the accuracy of Itrax CS- $\mu$ XRF. The Sr/Ca (cps/ma/cps/ma) ratio of ITRAX CS- $\mu$ XRF is typically two orders of magnitude greater than conventional XRF (Table 1). Such an offset is likely related to different excitation efficiencies of Sr and Ca. The orders of magnitude offset is likely a feature of previous Itrax

**Table 1**Sr/Ca measurements from contrasting analytical techniques.

Standard	Itrax CS-μXRF cps/mA/cps/mA	Conventional XRF mol/mol	Q-ICP-MS mol/mol
CAXS-1	$1.30-2.01 \times 10^{-2}$	$1.92 \times 10^{-4}$	$2.12 \times 10^{-4}$
CCXS-1	$3.70-5.88 \times 10^{-2}$	$5.30 \times 10^{-4}$	$5.67 \times 10^{-4}$
DAXS-1	$0.65-1.00 \times 10^{-2}$	$0.91 \times 10^{-4}$	$1.05 \times 10^{-4}$

studies, and has been previously reported where inter-methodological comparisons have been made e.g. Li et al. (2015) show an order of magnitude offset between Itrax Sr/Ca and ICP-OES Sr/Ca. However, Buckles and Rowe (2016), show little offset between their portable-XRF system and ICP-OES. This suggests that the Itrax offset is not inherent to XRF analysis but rather arises from incorrect calibration in the signal processing specific to this methodology.

Measurement of the three standards produces a linear fit which passes within error of a line scan  $2\sigma$  variability of each standard and  $<7.1\times10^{-6}$  mol/mol away from a zero intercept (Fig. 4a). The measurement of all three standards per run creates a linear correction used to correct  $(^{cps/mA}/_{cps/mA})$  to mol/mol in sample scans. After correction of ITRAX Sr/Ca to mol/mol, a consistent offset can still sometimes be observed between results on different days (Fig. 4c, d). However, this offset is much smaller than before and is small relative to the size of signal variability especially considering the stoichiometric assumptions in the conventional XRF methodology: 5.4% offset of signal in the stalagmite line scan in Figs. 4c and 6.7% offset in the stalagmite line scan in Fig. 4d, relative to a factor of seven variability in signal. We conclude that, while not accounting for all run to run variation, correcting the Itrax CS- $\mu$ XRF Sr/Ca  $(^{cps/mA}/_{cps/mA})$  to mol/mol using the in-house standards does provide a significant improvement.

The use of our correction is validated by comparison with Q-ICP-MS The difference between the standards measured using conventional XRF and Q-ICP-MS molar ratios varies by an average of 10%. Again, a 10% offset is small compared to factor of seven variation in Sr/Ca in the speleothem dataset. This independent measure of Sr/Ca shows that correction of Itrax Sr/Ca ( $^{\text{cps/mA}}/_{\text{cps/mA}}$ ) to mol/mol produces accurate results comparable with other methodologies (see Section 3.3 for further comparison).

To test the homogeneity of the in-house standards, line scans rather than spot analyses were conducted. After conversion to mol/mol the standards show an average  $2\sigma$  error < 9% of the signal for DAXS-1, 4% for CAXS-1, and 4% for CCXS-1 (Fig. 4b). Spot analyses are therefore not recommended for CS- $\mu$ XRF; line scans will therefore produce more accurate results when correcting samples Sr/Ca ratios.

In certain situations, it may be more useful to compare Sr concentration (ppm) than Sr/Ca ratio (Fig. 5). Calibration curves derived from the in-house standards measured using traditional XRF also allow the conversion of Sr counts to concentration. Similar to the process of Sr/Ca correction, a linear fit to the three standards passes within error of a line scan  $2\sigma$  variability of each standard and < 220 cps/mA away from a zero intercept. Converting speleothem derived Sr counts to ppm run on different days can still produce a consistent offset between concentrations on different days (Fig. 5c, d).

#### 3.3. Comparison with Q-ICP-MS

In Section 3.2 we demonstrated that our in-house standards, when measured on conventional pellet-based XRF, produce similar magnitude results to Q-ICP-MS, and therefore can be used to correct Itrax XRF measurements to more accurate values. Here we provide a more detailed comparison of a short speleothem transect measured using Itrax and Q-ICP-MS.

Once corrected, the Sr/Ca results produced by Itrax CS-µXRF are very similar to those from Q-ICP-MS: absolute offset between the two

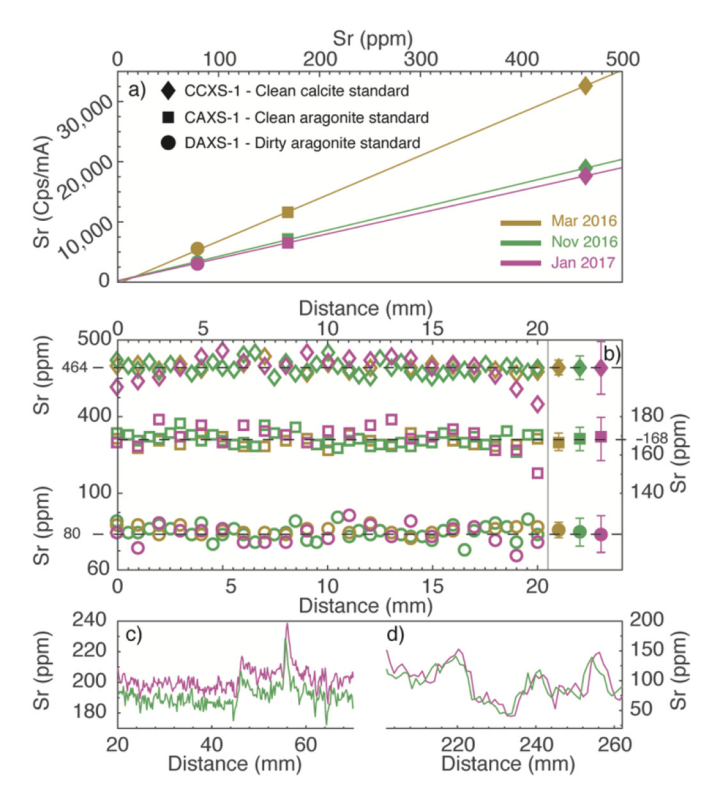


Fig. 5. Conversion of Sr (Cps/mA) to concentration (ppm) using in-house carbonate matrix standards measured on conventional XRF. a) Sr counts measured on the Itrax versus Sr concentration measured using conventional XRF. b) Line scan measurements of in-house standards testing standard homogeneity. Open symbols indicate line scans, closed symbols show the mean of each line scan with  $2\sigma$  error bars. c) Inter-run variability of Sr (ppm) concentrations on the same sections of stalagmite AB2 as Fig. 4. In all panels a dark yellow color represents the machine run during March 2016, green, November 2016, and purple, January 2017. Diamonds indicate measurements of the in-house standard CCXS-1, squares, CAXS-1, and circles, DAXS-1. (For interpretation of the references to color in this figure legend, the reader is referred to the web version of this article.)

records is just  $0.8\,\mu mol/mol$  or 0.5% of the range of variability. The timing of peaks and troughs is comparable between the two records, despite the difficulty in alignment from analyses being conducted on opposing stalagmite faces (Fig. 6a). The Q-ICP-MS Sr/Ca results produces higher peaks and deeper troughs (more variability) than the Itrax, suggesting a higher sensitivity of the Q-ICP-MS technique or greater spatial averaging by the Itrax. Linearly interpolating the Itrax results to Q-ICP-MS sample depths allows a correlation to be calculated at above 95% significance (Fig. 6b). The reduced major axis regression line between the two methods does not match the 1:1 line, likely due to the peak/trough mismatch described above, rather than the interpolation technique. The good match between the two techniques provides confidence that corrected Itrax CS- $\mu$ XRF accurately records speleothem Sr/Ca, but that further work is necessary to understand differences in sensitivity between the two methods.

#### 4. Discussion

#### 4.1. Itrax as a tool for determining mineralogy

Variability in the Sr/Ca ratio of stalagmite AB2 parallels changes in the speleothem mineralogy with a  $3 \times$  change in Sr/Ca between aragonite ( $\sim$ 0.015) and calcite ( $\sim$ 0.005) sections, as determined by 21 XRD measurements (Scroxton et al., 2017). Abrupt changes in the Sr/Ca ratio occur precisely at boundaries between the two carbonate polymorphs (Fig. 7). The size of the change is greater than any intra-

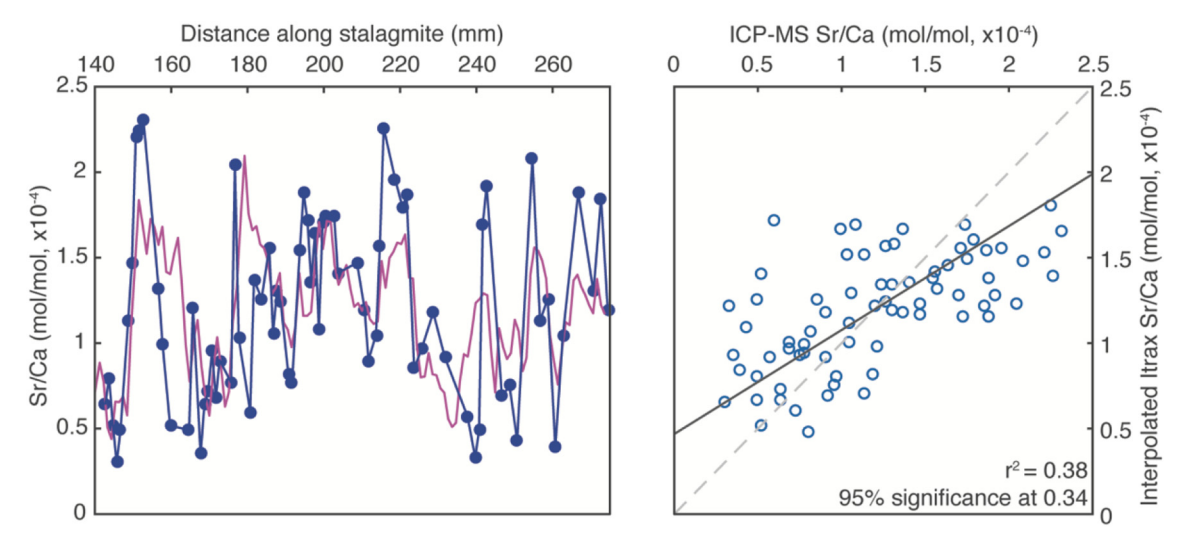


Fig. 6. Comparison of Sr/Ca ratios produced by Itrax CS-µXRF and ICP-MS. a) Line scan comparison of Itrax Sr/Ca at continuous 1 mm resolution (purple line) and ICP-MS Sr/Ca conducted on powder samples (blue filled circles connected by blue line) on the same section of stalagmite AB2. The resolution of the ICP-MS powders is nominally 1 mm, but multiple samples are missing as there was insufficient powder after prior stable isotope analyses. b) scatter plot of Sr/Ca results, with Itrax Sr/Ca linearly interpolated to the same depths as ICP-MS samples (open circles). Reduced major axis regression shown by dark grey line, 1:1 fit by light grey dashed line. (For interpretation of the references to color in this figure legend, the reader is referred to the web version of this article.)

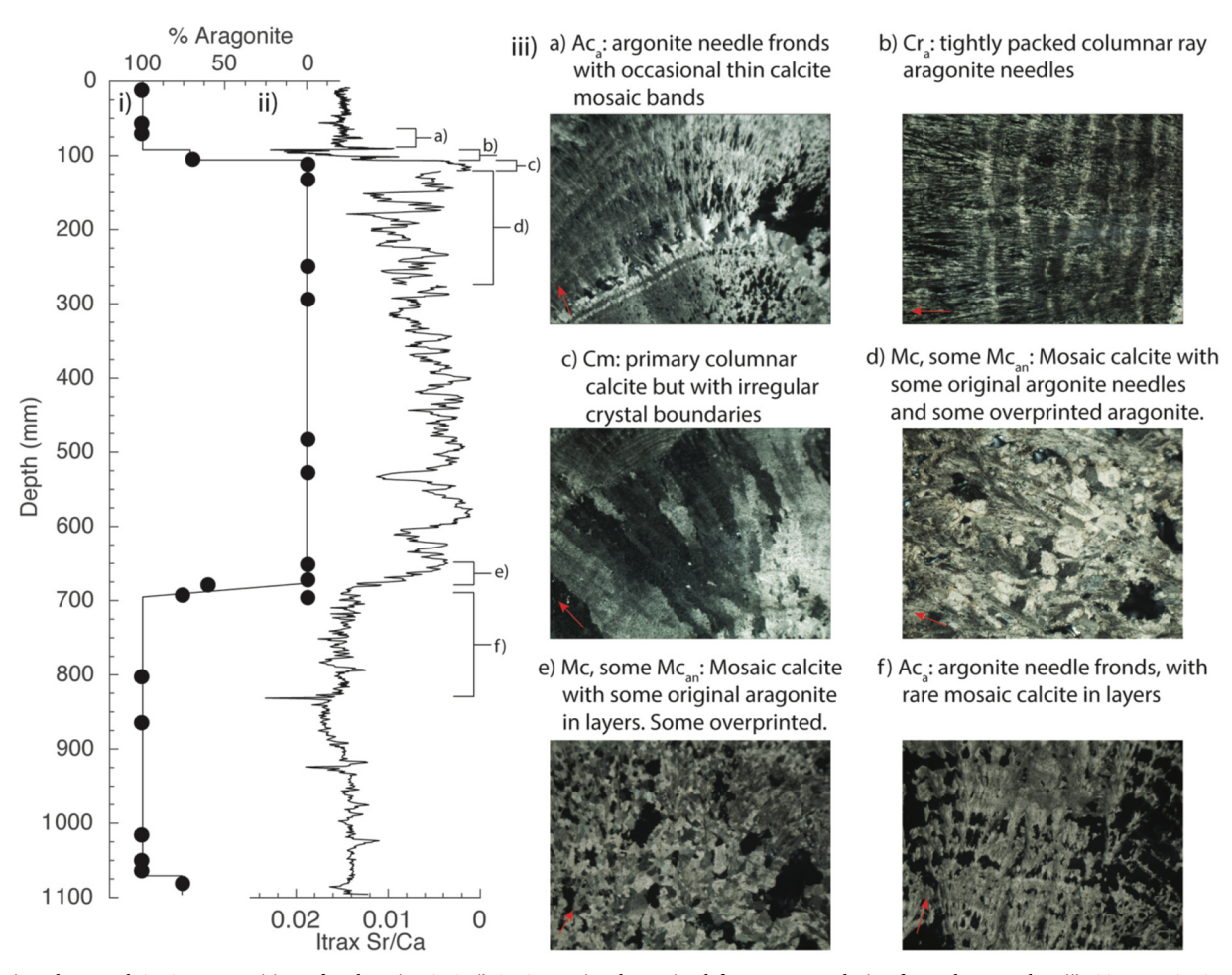


Fig. 7. Mineralogy and Sr/Ca composition of stalagmite AB2. i) % Aragonite determined from XRD analysis of powder samples. ii) CS-μXRF Sr/Ca ratio. iii) Microscope photographs of petrographic thin sections under cross polarized light from different type mineralogies in AB2. Red arrows indicate approximate growth direction. a, e, f) magnified so that each image is approximately 16 mm across. b, c, d) magnified so that each image is approximately 4 mm across. (For interpretation of the references to color in this figure legend, the reader is referred to the web version of this article.)

mineralogy variability suggesting that the ratio change likely results from the mineralogical change, as opposed to climatic or solutional variability that might have caused the mineralogical change. Theoretical considerations indicate this behavior arises from the incorporation of the Sr<sup>2+</sup> cation into the carbonate matrix. The orthorhombic structure of aragonite creates a larger cation site than the trigonal calcite structure, allowing easier substitution of cations larger than calcium into the lattice. As a result, Sr has a distribution coefficient well below 1 in speleothem calcite (Day and Henderson, 2013; Huang and Fairchild, 2001), and likely above 1 in speleothem aragonite (Wassenburg et al., 2016). Strontium is therefore preferentially incorporated into aragonite from speleothem drip waters but excluded from calcite. Thus, the Sr/Ca ratio is sensitive to mineralogy, and CS-μXRF can serve as a rapid way of determining the precise location of calcite-aragonite transitions in mixed mineralogy speleothems.

Visual inspection of the fabric of stalagmite AB2 using thin sections analyzed under a light microscope confirms the broad pattern of high Sr/Ca in the primary aragonite sections of stalagmite, and lower Sr/Ca in calcite sections. Identification of local replacement of aragonite by secondary calcite may also align with the smaller scale variability in Sr/Ca. This suggests that the recrystallization process interferes with Sr concentration, but does not fully convert the trace element signature (Domínguez-Villar et al., 2017). This prevents a full paleoclimatic interpretation of the Sr/Ca record of stalagmite AB2.

Between 101 and 106 mm in stalagmite AB2 there is a short section of mixed mineralogy, measured as 71% aragonite. Part of this section has a Sr/Ca ratio between 0.009 and 0.013, suggesting that the Sr/Ca of such sections may respond proportionally to the amount of aragonite versus calcite present, likely due to recrystallization (Perrin et al., 2014). However, between 94 and 101 mm there is a section of very high Sr/Ca between 0.016 and 0.023, higher than during the 100% aragonite sections. Visual inspection of this section indicates tightly packed columnar ray aragonite needles (Fig. 7b). We hypothesize that the cause is a shift in the style of prior carbonate precipitation above the stalagmite. Prior calcite precipitation (PCP) enriches the solution with respect to the Sr ion, and therefore increases the Sr concentration in the speleothem. Prior aragonite precipitation (PAP) depletes the solution, and therefore decreases the Sr concentration in the speleothem. Therefore consecutive mineralogies of 1) PCP above a calcite speleothem followed by, 2) PCP above an aragonite speleothem, and finally, 3) PAP above an aragonite speleothem would produce a Sr/Ca progression of 1) low Sr/ Ca, 2) very high Sr/Ca, 3) high Sr/Ca in the stalagmite. This matches the observed Sr/Ca ratio progression in the stalagmite during this section.

Further this is a logical progression during a drying trend. Lateral changes in mineralogy have been frequently observed in stalagmite textures due to changing solution chemistry during precipitation (Wassenburg et al., 2012). Therefore, it is feasible that mineralogical fronts could move upstream (downstream) during a drying (wetting) trend. A simultaneous increase in (mineralogy corrected)  $\delta^{18}{\rm O}$  (Scroxton et al., 2017) i.e. drying conditions, adds support to the idea of a drying trend producing this highly variable but mineralogically controlled Sr/Ca progression.

#### 4.2. Itrax as a tool for speleothem paleoclimatology

Sr/Ca has become a widely-used proxy in speleothem paleoclimatology. It is frequently interpreted as recording local rainfall amount via the mechanism of karst water residence time altering the degree of prior carbonate precipitation above the stalagmite (Fairchild et al., 2000; Johnson et al., 2006; Sinclair et al., 2012). Additional mechanisms may also influence Sr concentrations in speleothems, raising a degree of caution to simple interpretations. The Sr/Ca of the dripwater can be influenced by changes to the supply of non-host rock strontium sources such as sea salt, dust or volcanic ash weathering (Ayalon et al., 1999; Banner et al., 1996; Goede, 1998), the degree of dolomite

dissolution (Chou et al., 1989; Cowell and Ford, 2011), and the amount of incongruous dissolution (Busenberg and Niel Plummer, 1985). Strontium incorporation into the carbonate lattice can be hindered by the presence of other trace elements which outcompete strontium during infiltration events (Borsato et al., 2007; Smith et al., 2009). In theory, the degree of Sr incorporation into the carbonate lattice is influenced by growth rate, but several studies suggest this may only be at very low or very high growth rates (Gabitov and Watson, 2006; Wassenburg et al., 2016), or that the effect is so small that only very large changes in growth rate can override the influence of changing solution chemistry (Huang and Fairchild, 2001; Treble et al., 2003).

Despite these caveats, Sr/Ca is often used as a precipitation proxy alongside Mg/Ca. However, it is not possible to measure Mg/Ca using CS-µXRF due to the attenuation of secondary X-rays in the air gap. XRF systems that use a vacuum system are able to detect Mg above background, e.g. bench-top XRF (de Winter et al., 2017), as are soft X-ray SR-µXRF beams, but these methods are more destructive to the speleothem, requiring much smaller samples to fit inside vacuum chambers.

Our final test compares two stalagmite time series to see if Itrax Sr/Ca produces a similar climatic interpretation to a record produced using other methods. A direct comparison of Sr/Ca to Sr/Ca is not appropriate here as speleothem trace elements from the same cave can appear very different due to variability between drip-site chemistry. Instead we compare an Itrax Sr/Ca times series with a six-proxy principal component analysis time series from the same cave.

The top 250 mm of stalagmite LR06-B3 from Liang Luar, Flores, Indonesia was run at 0.2 mm resolution using a Cr tube in an Itrax at the Australian Nuclear Science and Technology Organisation. The top 250 mm covers approximately the last 2300 years. The corrected Sr/Ca record is tentatively interpreted as showing the degree of prior calcite precipitation above the cave, related to changes in rainfall amount.

We compare LR06-B3 Sr/Ca with LLPC1, the first component of a principial component analysis covering the last 2000 years (Griffiths

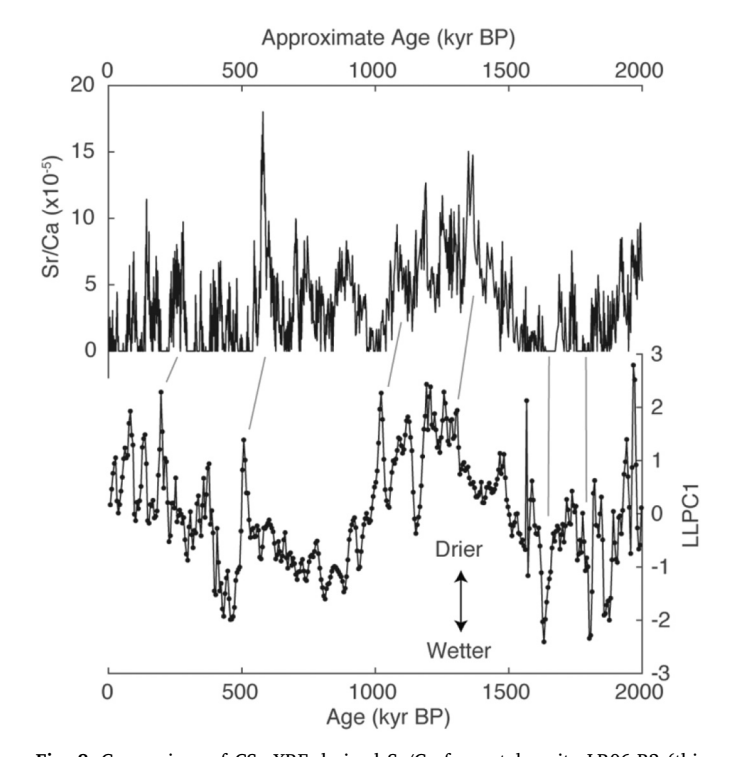


Fig. 8. Comparison of CS- $\mu$ XRF derived Sr/Ca from stalagmite LR06-B3 (this study) with principal component analysis of stable isotope and trace elements of stalagmites LR06-B1 and LR06-B3 (Griffiths et al., 2016). Due to uncertainty in the relative depth models of the two techniques, dotted lines indicate potential peak and trough matches.

Table 2
Summary of main strengths and weaknesses of CS-µXRF analysis of speleothems.

Strengths	Weaknesses
Accurate: results comparable with Q-ICP-MS in both magnitude and variability (after standard correction)	High detection limits: an order of magnitude larger than other techniques
Rapid: preliminary results in as little as 10s per scan, precise results in 40s per scan. Minor sample preparation and little machine overhead time	Low energy resolution: prevents detection of elements with $K\alpha$ energies close to elements with significant weight %, see Ca below
Precise: reproducible Sr/Ca ratios with errors much less than typical signal magnitudes ( $\pm$ 5%)	Matrix interference: XRD peaks from carbonate crystal lattice present but detectable
Reproducible: reproducibility of ratios in intra-run tests ( $< 10\%$ )	Dominance of calcium: high Kα and Kβ peaks, sum and escape lines obscure potentially useful elements
High Resolution: 0.2 mm in this study setup, up to 0.1 mm on some Itrax devices	Wide beam width: requires 16 mm flat surface with few significant lateral changes in growth axis
Non-destructive: no powders or ablation. Itrax system allows samples up to 1750x105x75mm	Lack of fine spatial control: no fine scale lateral adjustments and no mapping capabilities
Competitively priced: around \$2.50 per data point at 40s count time (approximate cost at UMass)	Sensitive to surface heterogeneity: requires wide flat analysis surface with no prior sampling

et al., 2016) (Fig. 8). LLPC1 is comprise of six proxies from two speleothems:  $\delta^{18}$ O and  $\delta^{13}$ C from isotope ratio mass spectrometry of LR06-B3,  $\delta^{18}$ O and  $\delta^{13}$ C from isotope ratio mass spectrometry of coeval stalagmite LR06-B1 (Griffiths et al., 2009), and Mg/Ca and Sr/Ca ratios measured by solution ICP-AES on LR06-B1 (Griffiths et al., 2010). The  $\delta^{13}$ C, Mg/Ca and Sr/Ca records heavily load onto the first principal component, LLPC1, while the two  $\delta^{18}$ O records did not significantly load onto LLPC1. LLPC1 was interpreted as the dominant karst hydrological signal seen in the  $\delta^{13}$ C, Mg/Ca and Sr/Ca records (Griffiths et al., 2016).

The two records show broad similarities in decadal to centennial variability. Both records indicate wetter conditions between 600 and 1000 CE and 1500–1800 CE and drier conditions between 1000 and 1400 CE and the 20th century. The CS-µXRF Sr/Ca record bottoms out with zero Sr counts recorded multiple times indicating the Sr concentration may be below the detection limits of the Itrax. During wet periods the solution reaching the stalagmite apparently did not have sufficient Sr to produce a signal that can be detected using CS-µXRF. The quoted detection limits for Sr in an Itrax using a Cr tube is 15 ppm, using a setup of a 100 s count time in a clay matrix. The detection limits for our crushed carbonate Sr standards are around 10 ppm. However, the precise detection limits for crystalline speleothems, which could vary with speleothem fabric, in this experimental setup are yet to be determined.

We acknowledge two limitations of our comparison between our Itrax results and LLPC1: first, as  $\delta^{13} C$  from LR06-B3 may be controlled by prior calcite precipitation, the two records may not be truly independent. Secondly, a precise age model of LR06-B3 is not possible due to the chronological difficulties arising from Itrax analysis on the opposite face, with restricted lateral movement to mimic the stable isotope transect, and a lack of distinguishing layer features in LR06-B3 to provide tie points. Because of this chronological uncertainty, and the autocorrelation of both times series, correlation between the two timeseries isn't statistically significant:  $t=0.8,\,t_{crit}=1.9$  for the comparison between CS- $\mu$ XRF and LLPC1, t=0.1.

#### 5. Conclusions and future directions of study

CS-µXRF is a promising technique for measuring trace elements in speleothems, providing a high resolution, reproducible, precise, rapid, largely non-destructive method for determining Sr/Ca ratios in speleothem carbonate. Sr/Ca can be used as a proxy for speleothem

mineralogy and paleohydrology. The strengths and weaknesses of the Itrax setup are summarized in Table 2. Work remains to understand the finer details of the methodology, particularly relating to the impact of the carbonate matrix, the effects of different X-ray tubes, Itrax machine settings, and the influence of surface roughness and crystallinity.

In this study, we have focused on a single element, Sr. CS-µXRF can record most elements heavier than aluminum, if in high enough abundance. However, the influence of X-ray diffraction peaks and calcium peaks upon individual elements needs to be further explored before reliable records can be produced. On a cautionary note, as analytical techniques for measuring trace elements in speleothems improve and become more widespread, further research is needed into the environmental significance of these elements to avoid overinterpretation. The behavior of many elements through the karst system needs to be better understood before reliable paleoclimate inferences can be drawn from new time series. As our understanding of physical and chemical karst processes increases it is likely that trace element concentrations in speleothems will become increasingly used as an alternative or as a supplement to stable isotope ratios for paleoenvironmental reconstructions. CS-µXRF therefore represents a valuable new tool in the ongoing process of determining past rainfall variability using speleothems.

#### Acknowledgements

The authors would like to thank Irit Tal for her help in the lab. Funding for the core scanner at UMass was provided by the National Science Foundation grant EAR-0949313 to JMR. Funding for analyses at ANSTO provided as part of Australian Research Council LIEF Grant LE100100141, Australian Institute of Nuclear Sciences & Engineering (AINSE) grant ALNGRA11165 and Australian Research Council Discovery grant DP0663274 to MKG. Fieldwork in Indonesia was carried out under LIPI research permit number 04057/SU/KS/2006.

#### References

Ayalon, A., Bar-Matthews, M., Kaufman, A., 1999. Petrography, strontium, barium and uranium concentrations, and strontium and uranium isotope ratios in speleothems as palaeoclimatic proxies: Soreq Cave, Israel. The Holocene 9, 715–722. http://dx.doi.org/10.1191/095968399673664163.

Banner, J.L., Musgrove, M., Asmerom, Y., Edwards, R.L., Hoff, J.A., 1996. High-resolution temporal record of Holocene ground-water chemistry: tracing links between climate and hydrology. Geology 24, 1049–1053. http://dx.doi.org/10.1130/0091-7613(1996)024<1049:HRTROH>2.3.CO;2.

- Badertscher, S., Borsato, A., Frisia, S., Cheng, H., Edwards, R.L., Tuysuz, O., Fleitmann, D., 2014. Speleothems as sensitive recorders of volcanic eruptions the Bronze Age Minoan eruption recorded in a stalagmite from Turkey. Earth Planet. Sci. Lett. 392, 58–66.
- Blyth, A.J., Hartland, A., Baker, A., 2016. Organic proxies in speleothems new developments, advantages and limitations. Quat. Sci. Rev. 149, 1–17. http://dx.doi.org/10.1016/j.quascirev.2016.07.001.
- Baldini, J.U.L., McDermott, F., Fairchild, I.J., 2006. Spatial variability in cave drip water hydrochemistry: implications for stalagmite paleoclimate records. Chem. Geol. 235, 390–404.
- Borsato, A., Frisia, S., Fairchild, I.J., Somogyi, A., Susini, J., 2007. Trace element distribution in annual stalagmite laminae mapped by micrometer-resolution X-ray fluorescence: implications for incorporation of environmentally significant species. Geochim. Cosmochim. Acta 71, 1494–1512. http://dx.doi.org/10.1016/j.gca.2006. 12.016
- Brown, G.E., Sturchio, N.C., 2002. An overview of synchrotron radiation applications to low temperature geochemistry and environmental science. Rev. Mineral. Geochem. 49, 1–115. http://dx.doi.org/10.2138/gsrmg.49.1.1.
- Buckles, J., Rowe, H.D., 2016. Development and optimization of microbeam X-ray fluorescence analysis of Sr in speleothems. Chem. Geol. 426, 28–32. http://dx.doi. org/10.1016/j.chemgeo.2016.02.003.
- Busenberg, E., Niel Plummer, L., 1985. Kinetic and thermodynamic factors controlling the distribution of SO 3 2 – and Na+ in calcites and selected aragonites. Geochim. Cosmochim. Acta 49, 713–725.
- Chappell, B.W., 1991. Trace element analysis of rocks by X-ray spectrometry. Adv. X-ray Anal. 263–276. http://dx.doi.org/10.1007/978-1-4615-3744-1\_28.
- Chou, L., Garrels, R.M., Wollast, R., 1989. Comparative study of the kinetics and mechanisms of dissolution of carbonate minerals. Chem. Geol. 78, 269–282. http://dx.doi.org/10.1016/0009-2541(89)90063-6.
- Cowell, D.W., Ford, D.C., 2011. Hydrochemistry of a dolomite karst: the Bruce Peninsula of Ontario. Can. J. Earth Sci. 17, 520–526. http://dx.doi.org/10.1139/e80-048.
- Croudace, I.W., Rindby, A., 2006. ITRAX: description and evaluation of a new multi-function X-ray core scanner. Geol. Soc. Lond. Spec. Publ. 267, 51–63. http://dx.doi.org/10.1144/gsl.sp.2006.267.01.04.
- Cruz Jr., F.W., Burns, S.J., Jercinovic, M., Karmann, I., Sharp, W.D., Vuille, M., 2007. Evidence of rainfall variations in southern Brazil from trace element ratios (Mg/Ca and Sr/Ca) in a Late Pleistocene stalagmite. Geochim. Cosmochim. Acta 71, 2250–2263. http://dx.doi.org/10.1016/j.gca.2007.02.005.
- Day, C.C., Henderson, G.M., 2013. Controls on trace-element partitioning in cave-analogue calcite. Geochim. Cosmochim. Acta 120, 612–627. http://dx.doi.org/10.1016/i.gca.2013.05.044.
- Domínguez-Villar, D., Krklec, K., Pelicon, P., Fairchild, I.J., Cheng, H., Edwards, L.R., 2017. Geochemistry of speleothems affected by aragonite to calcite recrystallization – potential inheritance from the precursor mineral. Geochim. Cosmochim. Acta 200, 310–329. http://dx.doi.org/10.1016/j.gca.2016.11.040.
- Fairchild, I.J., Treble, P.C., 2009. Trace elements in speleothems as recorders of environmental change. Quat. Sci. Rev. 28, 449–468. http://dx.doi.org/10.1016/j.guascirev.2008.11.007
- Fair-Child, I.J., Borsato, A., Tooth, A.F., Frisia, S., Hawkesworth, C.J., Huang, Y., McDermott, F., Spiro, B., 2000. Controls on trace element (Sr-Mg) compositions of carbonate cave waters: implications for speleothem climatic records. Chem. Geol. 166. 255-269.
- Fernandez, D.P., Gagnon, A.C., Adkins, J.F., 2011. An isotope dilution ICP-MS method for the determination of Mg/Ca and Sr/Ca ratios in calcium carbonate. Geostand. Geoanal. Res. 35, 23–37. http://dx.doi.org/10.1111/j.1751-908X.2010.00031.x.
- Finné, M., Kylander, M., Boyd, M., Sundqvist, H., Löwemark, L., 2015. Can XRF scanning of speleothems be used as a non-destructive method to identify paleoflood events in caves? Int. J. Speleol. 44, 17–23. http://dx.doi.org/10.5038/1827-806x.44.1.2.
- Frisia, S., Borsato, A., Fairchild, I.J., Susini, J., 2005. Variations in atmospheric sulphate recorded in stalagmites by synchrotron micro-XRF and XANES analyses. Earth Planet. Sci. Lett. 235, 729–740. http://dx.doi.org/10.1016/j.epsl.2005.03.026.
- Frisia, S., Borsato, A., Susini, J., 2008. Synchrotron radiation applications to past volcanism archived in speleothems: an overview. J. Volcanol. Geotherm. Res. 177, 96–100. http://dx.doi.org/10.1016/j.jvolgeores.2007.11.010.
- Frisia, S., Borsato, A., Drysdale, R.N., Paul, B., Greig, A., Cotte, M., 2012. A re-evaluation of the palaeoclimatic significance of phosphorus variability in speleothems revealed by high-resolution synchrotron micro XRF mapping. Clim. Past 8, 2039–2051. http://dx.doi.org/10.5194/cp-8-2039-2012.
- Gabitov, R.I., Watson, E.B., 2006. Partitioning of strontium between calcite and fluid. Geochem. Geophys. Geosyst. 7. http://dx.doi.org/10.1029/2005GC001216.
- Goede, A., 1998. Aeolian contribution to strontium and strontium isotope variations in a Tasmanian speleothem. Chem. Geol. 149, 37–50. http://dx.doi.org/10.1016/S0009-2541(98)00035-7.
- Griffiths, M.L., Drysdale, R.N., Gagan, M.K., Zhao, J.-X., Ayliffe, L.K., Hellstrom, J.C., Hantoro, W.S., Frisia, S., Feng, Y., Cartwright, I., Pierre, E.S., St Pierre, E., Fischer, M.J., Suwargadi, B.W., 2009. Increasing Australian-Indonesian monsoon rainfall linked to early Holocene sea-level rise. Nat. Geosci. 2, 636–639. http://dx.doi.org/ 10.1038/NGE0605.
- Griffiths, M.L., Drysdale, R.N., Gagan, M.K., Frisia, S., Zhao, J.-X., Ayliffe, L.K., Hantoro, W.S., Hellstrom, J.C., Fischer, M.J., Feng, Y.X., Suwargadi, B.W., 2010. Evidence for Holocene changes in Australian-Indonesian monsoon rainfall from stalagmite trace element and stable isotope ratios. Earth Planet. Sci. Lett. 292, 27–38. http://dx.doi.org/10.1016/j.epsl.2010.01.002.
- Griffiths, M.L., Drysdale, R.N., Gagan, M.K., Gagan, M.K., Zhao, J.-X., Hellstrom, J.C., Hellstrom, J.C., Ayliffe, L.K., Ayliffe, L.K., Hantoro, W.S., Hantoro, W.S., 2013. Abrupt increase in east Indonesian rainfall from flooding of the Sunda Shelf

9500 years ago. Quat. Sci. Rev. 74, 273-279.

- Griffiths, M.L., Kimbrough, A.K., Gagan, M.K., Drysdale, R.N., Cole, J.E., Johnson, K.R., Zhao, J.-X., Cook, B.I., Hellstrom, J.C., Hantoro, W.S., 2016. Western Pacific hydroclimate linked to global climate variability over the past two millennia. Nat. Commun. 7. http://dx.doi.org/10.1038/ncomms11719.
- Huang, Y., Fairchild, I.J., 2001. Partitioning of Sr2+ and Mg2+ into calcite under karst-analogue experimental conditions. Geochim. Cosmochim. Acta 65, 47–62. http://dx.doi.org/10.1016/S0016-7037(00)00513-5.
- Jamieson, R.A., Baldini, J.U.L., Brett, M.J., Taylor, J., Ridley, H.E., Ottley, C.J., Prufer, K.M., Wassenburg, J.A., Scholz, D., Breitenbach, S.F.M., 2016. Intra- and inter-annual uranium concentration variability in a Belizean stalagmite controlled by prior aragonite precipitation: a new tool for reconstructing hydro-climate using aragonitic speleothems. Geochim. Cosmochim. Acta 190, 332–346. http://dx.doi.org/10.1016/j.gra. 2016.06.037
- Jarvis, S., Croudace, I.W., Rothwell, R.G., 2015. Parameter optimisation for the ITRAX core scanner. In: Croudace, I.W., Rothwell, R.G. (Eds.), Micro-XRF Studies of Sediment Cores. Micro-XRF Studies of Sediment ..., pp. 535–562. http://dx.doi.org/10.1007/978-94-017-9849-5 22.
- Johnson, K.R., Ingram, B.L., 2004. Spatial and temporal variability in the stable isotope systematics of modern precipitation in China: implications for paleoclimate reconstructions. Earth Planet. Sci. Lett. 220, 365–377. http://dx.doi.org/10.1016/ S0012-821X(04)00036-6.
- Johnson, K.R., Hu, C., Belshaw, N.S., Henderson, G.M., 2006. Seasonal trace-element and stable-isotope variations in a Chinese speleothem: the potential for high-resolution paleomonsoon reconstruction. Earth Planet. Sci. Lett. 244, 394–407. http://dx.doi. org/10.1016/j.epsl.2006.01.064.
- Kanner, L.C., Burns, S.J., Cheng, H., Edwards, R.L., 2012. High-latitude forcing of the south American summer monsoon during the last glacial. Science 335, 570–573. http://dx.doi.org/10.1126/science.1213397.
- Kuczumow, A., Genty, D., Chevallier, P., Nowak, J., Ro, C.-U., 2003. Annual resolution analysis of a SW-France stalagmite by X-ray synchrotron microprobe analysis. Spectrochim. Acta B At. Spectrosc. 58, 851–865. http://dx.doi.org/10.1016/S0584-8547(03)00022-3.
- Kuczumow, A., Genty, D., Chevallier, P., Nowak, J., 2005. X-ray and electron microprobe investigation of the speleothems from Godarville tunnel. X-Ray Spectrom. 34, 502–508. http://dx.doi.org/10.1002/xrs.877.
- Lachniet, M.S., 2009. Climatic and environmental controls on speleothem oxygen-isotope values. Quat. Sci. Rev. 28, 412–432. http://dx.doi.org/10.1016/j.quascirev.2008.10. 021.
- Lachniet, M.S., 2015. Are aragonite stalagmites reliable paleoclimate proxies? Tests for oxygen isotope time-series replication and equilibrium. GSA Bull. 127, 1521–1533. http://dx.doi.org/10.1130/B31161.1.
- LeGrande, A.N., Schmidt, G.A., 2006. Global gridded data set of the oxygen isotopic composition in seawater. Geophys. Res. Lett. 33, 15833. http://dx.doi.org/10.1029/ 2006GL026011.
- LeGrande, A.N., Schmidt, G.A., 2009. Sources of Holocene variability of oxygen isotopes in paleoclimate archives. Clim. Past 5, 441–455. http://dx.doi.org/10.5194/cp-5-441-2009
- Li, H.-C., Zhao, M., Tsai, C.-H., Mii, H.-S., Chang, Q., Wei, K.-Y., 2015. The first high-resolution stalagmite record from Taiwan: climate and environmental changes during the past 1300 years. J. Asian Earth Sci. 114, 574–587. http://dx.doi.org/10.1016/j.iseaes.2015.07.025.
- Norrish, K., Chappell, B.W., 1967. X-ray fluorescence spectrography. In: Zussman, J. (Ed.), Physical Methods in Determinative Mineralogy, pp. 161–214.
- Orland, I.J., Burstyn, Y., Bar-Matthews, M., Kozdon, R., Ayalon, A., Matthews, A., Valley, J.W., 2014. Seasonal climate signals (1990–2008) in a modern Soreq Cave stalagmite as revealed by high-resolution geochemical analysis. Chem. Geol. 363, 322–333. http://dx.doi.org/10.1016/j.chemgeo.2013.11.011.
- Perrin, C., Prestimonaco, L., Servelle, G., Tilhac, R., Maury, M., Cabrol, P., 2014. Aragonite-calcite speleothems: identifying original and diagenetic features. J. Sediment. Res. 84, 245–269.
- Ramsey, M.H., Potts, P.J., Webb, P.C., Watkins, P., Watson, J.S., Coles, B.J., 1995. An objective assessment of analytical method precision: comparison of ICP-AES and XRF for the analysis of silicate rocks. Chem. Geol. 124, 1–19. http://dx.doi.org/10.1016/0009-2541(95)00020-M.
- Rhodes, J.M., Vollinger, M.J., 2004. Composition of basaltic lavas sampled by phase-2 of the Hawaii scientific drilling project: geochemical stratigraphy and magma types. Geochem. Geophys. Geosyst. 5. http://dx.doi.org/10.1029/2002GC000434.
- Risi, C., Bony, S., Vimeux, F., 2008. Influence of convective processes on the isotopic composition ( $\delta$ 180 and  $\delta$ D) of precipitation and water vapor in the tropics: 2. Physical interpretation of the amount effect. J. Geophys. Res. 113, D19306. http://dx.doi.org/10.1029/2008JD009943.
- Rozanski, K., Araguás-Araguás, L., Gonfiantini, R., 1993. Isotopic patterns in modern global precipitation. Geophys. Monogr. Ser. 78, 1–36.
- Sinclair, D.J., Banner, J.L., Taylor, F.W., Partin, J.W., Jenson, J., Mylroie, J., Goddard, E., Quinn, T., Jocson, J., Miklavič, B., 2012. Magnesium and strontium systematics in tropical speleothems from the Western Pacific. Chem. Geol. 294–295, 1–17. http:// dx.doi.org/10.1016/j.chemgeo.2011.10.008.
- Scroxton, N., Burns, S.J., McGee, D., Hardt, B., Godfrey, L.R., Ranivoharimanana, L., Faina, P., 2017. Hemispherically in-phase precipitation variability over the last 1700 years in a Madagascar speleothem record. Quat. Sci. Rev. 164, 25–36. http://dx.doi.org/10.1016/j.quascirev.2017.03.017.
- Smith, C.L., Fairchild, I.J., Spötl, C., Frisia, S., Borsato, A., Moreton, S.G., Wynn, P.M., 2009. Chronology building using objective identification of annual signals in trace element profiles of stalagmites. Quat. Geochronol. 4, 11–21. http://dx.doi.org/10.1016/j.quageo.2008.06.005.

Tan, L., Cai, Y., An, Z., Cheng, H., Shen, C.-C., Breitenbach, S.F.M., Gao, Y., Edwards, R.L., Zhang, H., Du, Y., 2015. A Chinese cave links climate change, social impacts, and human adaptation over the last 500 years. Sci. Rep. 5. http://dx.doi.org/10.1038/srep12284.

- Treble, P.C., Shelley, J., Chappell, J., 2003. Comparison of high resolution sub-annual records of trace elements in a modern (1911-1992) speleothem with instrumental climate data from southwest Australia. Earth Planet. Sci. Lett. 216, 141–153. http://dx.doi.org/10.1016/S0012-821X(03)00504-1.
- Verheyden, S., Keppens, E., Fairchild, I.J., McDermott, F., Weis, D., 2000. Mg, Sr and Sr isotope geochemistry of a Belgian Holocene speleothem: implications for paleoclimate reconstructions. Chem. Geol. 169, 131–144. http://dx.doi.org/10.1016/S0009-2541(00)00299-0.
- Wassenburg, J.A., Immenhauser, A., Richter, D.K., Jochum, K.P., Fietzke, J., Deininger, M., Goos, M., Scholz, D., Sabaoui, A., 2012. Climate and cave control on Pleistocene/Holocene calcite-to-aragonite transitions in speleothems from Morocco: elemental and isotopic evidence. Geochim. Cosmochim. Acta 92, 23–47. http://dx.doi.org/10.1016/j.gca.2012.06.002.
- Wassenburg, J.A., Scholz, D., Jochum, K.P., Cheng, H., Oster, J., Immenhauser, A., Richter, D.K., Häger, T., Jamieson, R.A., Baldini, J.U.L., Hoffmann, D., Breitenbach,

- S.F.M., 2016. Determination of aragonite trace element distribution coefficients from speleothem calcite–aragonite transitions. Geochim. Cosmochim. Acta 190, 347–367. http://dx.doi.org/10.1016/j.gca.2016.06.036.
- de Winter, N.J., Sinnesael, M., Makarona, C., Vansteenberge, S., Claeys, P., 2017. Trace element analyses of carbonates using portable and micro-X-ray fluorescence: performance and optimization of measurement parameters and strategies. J. Anal. At. Spectrom. 55, 863. http://dx.doi.org/10.1039/C6JA00361C.
- Wu, J.Y., Wang, Y.J., Cheng, H., Kong, X.G., Liu, D.B., 2012. Stable isotope and trace element investigation of two contemporaneous annually-laminated stalagmites from northeastern China surrounding the "8.2 ka event". Clim. Past 8, 1497–1507.
- Wynn, P.M., Borsato, A., Baker, A., Frisia, S., Miorandi, R., Fairchild, I.J., 2012. Biogeochemical cycling of sulphur in karst and transfer into speleothem archives at Grotta di Ernesto, Italy. Biogeochemistry 114, 255–267. http://dx.doi.org/10.1007/ s10533-012-9807-z.
- Wynn, P.M., Fairchild, I.J., Spötl, C., Hartland, A., Mattey, D., Fayard, B., Cotte, M., 2014. Synchrotron X-ray distinction of seasonal hydrological and temperature patterns in speleothem carbonate. Environ. Chem. 11, 28–36. http://dx.doi.org/10.1071/ FNI 3082